



POLITECNICO
MILANO 1863

**SCUOLA DI INGEGNERIA INDUSTRIALE
E DELL'INFORMAZIONE**

EXECUTIVE SUMMARY OF THE THESIS

Inter-satellite Link-Based One-Way Ranging for Spacecraft Formation Flying

LAUREA MAGISTRALE IN SPACE ENGINEERING - INGEGNERIA SPAZIALE

Author: GIORGIA CIRILLI

Advisor: PROF. MICHÈLE ROBERTA LAVAGNA

Co-advisor: FRANCESCO DE CECIO, ENRICO BELLONI

Academic year: 2023-2024

1. Introduction

The increasing use of distributed satellite systems for Earth observation, geolocation, and deep-space exploration has highlighted the need for autonomous and precise relative navigation techniques. This shift has been driven by spacecraft miniaturization, leading to the rise of CubeSats and small satellites. Consequently, mission strategies now emphasize low-cost, scalable, and rapidly deployable constellations, reshaping space-based system design and operation [3].

In such scenarios, spacecraft must autonomously manage navigation processes onboard, from generating and exchanging relative measurements to state estimation. This necessitates an inter-satellite communication link to facilitate navigation data exchange for accurate positioning and scientific data sharing.

This study models a radio-frequency inter-satellite link (ISL) for one-way ranging, aiming to enhance real-time relative navigation in satellite formations. It examines how sampling frequency, carrier and code tracking loops, and digital filtering techniques impact ranging accuracy.

2. Objectives

This research is structured around four main methodological objectives:

1. Develop a comprehensive RF-based ISL model by designing a detailed simulation framework that accurately represents the transmission and reception chain, while incorporating realistic propagation effects in a Low Earth Orbit (LEO) environment.
2. Adapt the GNSS receiver architecture for formation flying missions by refining the acquisition and tracking modules and optimizing discriminator selection.
3. Evaluate the impact of the sampling frequency on the tracking performance.
4. Assess the accuracy of the observables generated by the proposed ISL chain to perform one-way ranging

These objectives are tackled through numerical simulations and performance evaluations. Ultimately, this work aids in the development of the ISL one-way ranging system for the *VULCAIN* mission in LEO, fostering advancements in autonomous satellite navigation technologies.

3. GNSS fundamentals

GNSS determines user position through one-way ranging, where the receiver calculates the signal propagation time and multiplies it by the speed of light to estimate the relative distance [2].

Due to clock a-synchronization between the receiver and satellites, the actual measurement is the pseudorange, which includes an unknown clock bias. The pseudorange is expressed as: GNSS signals enable ranging through L-band transmissions (1-2 GHz), consisting of a unique ranging code for travel time measurement, a navigation message carrying satellite data, and a carrier wave modulated by both.

The receiver determines the signal travel time by correlating the incoming signal with a locally generated replica. The maximum correlation peak identifies the time lag, which is then converted into the reception time. This enables precise pseudorange estimation, which is crucial for accurate GNSS positioning.

3.1. GNSS receiver state of technology

GNSS receivers process signals through key stages to extract position, velocity, and time information. The RF front-end filters, amplifies, and digitizes the signal before acquisition estimates the incoming code delay and Doppler frequency. Tracking then refines these estimates by maintaining signal lock through continuous updates to the code phase, carrier phase, and Doppler shift.

Once tracking is stable, the receiver extracts navigation data, demodulating the signal to retrieve ephemeris, clock bias, and almanac information for precise positioning in dynamic environments [2].

4. Inter-satellite link model implementation

The inter-satellite link is designed for relative navigation between CubeSats and covers transmission, propagation, and reception. The transmitter generates and modulates the signal using a PRN sequence, navigation message, and carrier, while the propagation medium introduces frequency shifts, carrier phase variations, and code delays due to relative motion. The receiver acquires, tracks, and processes the signal to re-

cover the navigation message and estimate the inter-satellite range.

4.0.1 Use of a Unique PRN Code

A single PRN sequence is utilized since the satellites alternate between transmission and reception. However, a Code Division Multiple Access scheme will be used if the number of cooperative platforms increases. This approach assigns a unique PRN code to each satellite, preventing mutual interference and ensuring efficient bandwidth allocation.

The ranging code is based on the GPS C/A code, chosen for its autocorrelation properties and robustness. It undergoes binary phase shift keying modulation, where the navigation message is combined with the PRN sequence using a modulo-2 operation, forming a direct-sequence spread spectrum[1]. The carrier wave, generated at X-band frequency, is multiplied by the modulated signal. An optimal modulation is exploited to ensure that phase transitions align with zero crossings of the carrier, minimizing spectral interference.

4.1. Intermediate Frequency Selection and Impact of Sampling Frequency

The receiver processes the incoming signal by down-converting it to an intermediate frequency, filtering it, and digitizing it at a carefully chosen sampling rate.

The intermediate frequency is carefully chosen to balance filter complexity, system noise, and computational efficiency. A higher IF increases sampling frequency demands, while a lower IF requires highly selective filtering stages, increasing hardware complexity and insertion losses. A trade-off is made to ensure optimal filtering while keeping system noise minimal.

The sampling frequency directly influences tracking resolution for code delay, carrier phase, and frequency estimation. Since the pseudorange is the primary observable for one-way ranging, its selection is guided by the chipping rate, ensuring compliance with the Nyquist criterion to prevent aliasing. However, the DLL discriminator can only track range variations within $\pm d$, where d is the early-late spacing. Beyond this limit, it becomes ineffective, meaning an excessively high sampling rate does not improve ac-

curacy but instead increases computational demand unnecessarily. Moreover, since the carrier frequency is significantly higher than the chipping rate, selecting the sampling frequency based solely on the code rate is expected to degrade carrier phase and frequency tracking performance.

4.2. Data Size Selection, Correlation, and Processing Time Constraints

The data size for acquisition is set based on navigation bit transitions, processing constraints, and acquisition reliability. A bit transition within the correlation window introduces destructive interference, corrupting acquisition results [1]. A data size of 1 ms is chosen to minimize this risk, ensuring that transitions occur outside the correlation window with 95% probability, at the cost of sacrificing the improved accuracy that could be achieved with longer data windows.

The correlation process is implemented using a Parallel Code Phase Search Algorithm, reducing computational demand. Unlike serial search methods, which individually evaluate all possible code shifts, this approach transforms the signals into the frequency domain, enabling faster acquisition.

4.3. Tracking Loop Implementation

The tracking architecture consists of a Delay Lock Loop (DLL), Phase Lock Loop (PLL), and Frequency Lock Loop (FLL) as presented in Figure 1.

The DLL aligns the PRN code using a Normalized Early-Minus-Late discriminator, which provides robust tracking independent of carrier phase variations and navigation bit transitions. $D_{\text{NEML}}^{\text{DLL}}[n] = \frac{\sqrt{I_E^2[n] + Q_E^2[n]} - \sqrt{I_L^2[n] + Q_L^2[n]}}{\sqrt{I_E^2[n] + Q_E^2[n]} + \sqrt{I_L^2[n] + Q_L^2[n]}}$.

The PLL corrects phase misalignment using a Costas discriminator, ensuring insensitivity to navigation bit transitions: $D_{\text{Costas}}^{\text{PLL}}[n] = \tan^{-1}\left(\frac{Q_p[n]}{I_p[n]}\right)$. The FLL stabilizes frequency tracking using a modified frequency discriminator, which accounts for the receiver's sampling frequency:

$D^{\text{FLL}}[n] = \frac{(\text{cross}) \times \text{sign}(\text{dot})}{H/f_s}$, where $\text{cross} = I_{P1}Q_{P2} - I_{P2}Q_{P1}$, $\text{dot} = I_{P1}I_{P2} + Q_{P1}Q_{P2}$. Here, H represents half of the total samples per iteration ($H = N/2 = f_s T_i/2$), ensuring

compatibility with the sampling rate.

4.4. Parallelization of Carrier Loops and Synchronization Considerations

The carrier tracking loop consists of separate but coupled PLL and FLL loops, each controlling a single local oscillator. This parallel architecture simplifies implementation, improves performance evaluation, and enables independent filter tuning.

While Costas loops can track both phase and frequency simultaneously, they require coherent integration, which introduces complexity and noise sensitivity. Instead, independent PLL and FLL loops provide more flexibility, allowing the frequency loop to assist the phase loop without compromising tracking accuracy.

A synchronization mechanism is implemented to prevent navigation bit transitions from interfering with tracking. A detection block identifies the first transition and aligns the correlation window accordingly. This ensures that bit transitions occur at the edge of correlation windows, maintaining accurate PRN code tracking and enabling seamless navigation message recovery.

4.5. Navigation Message Recovery

Once the DLL is locked, the navigation message is recovered by correlating the prompt replica over 20 ms intervals, ensuring synchronization with the 50 Hz navigation bit rate. This approach reduces errors caused by transitions during the code convergence process, ensuring accurate demodulation.

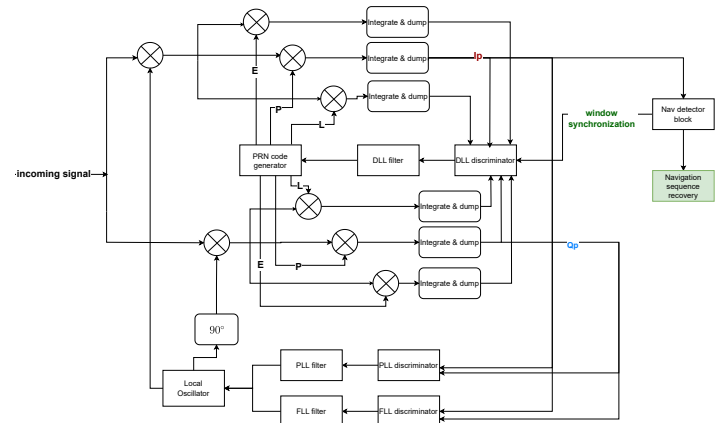


Figure 1: Complete tracking architecture.

5. Simulation Framework

The simulation framework is designed to evaluate the performance of ISL model, using the VULCAIN mission as a test case. The mission consists of two CubeSats maintaining a 300 km baseline in circular orbits at 400 km altitude, requiring precise one-way ranging for relative navigation. The ISL model extracts pseudorange observables, which are processed using an Extended Kalman Filter for accurate relative positioning. The relative motion of the spacecraft induces carrier phase, Doppler frequency shift, and code delay variations, which are derived from orbital mechanics. The acquisition stage for the VULCAIN mission is adapted by eliminating the frequency search. Given the small expected Doppler shift (± 8 Hz), carrier frequency correction is fully managed within the tracking stage.

Instead of searching for frequency offsets, the receiver only estimates the code delay. This modification reduces computational burden while still ensuring proper initialization of the DLL. Without an acquisition process over the code phase, the receiver would start tracking with a 2-chip misalignment, exceeding the DLL's pull-in range.

The intermediate frequency is set to 9.216 MHz, ensuring an efficient down-conversion process. The sampling frequency is chosen at 4.092 MHz to balance computational efficiency with accurate tracking performance. This ensures that the incoming ranging code is sampled at a rate that prevents aliasing and allows FFT-based acquisition.

The Early-Late Spacing for the DLL is set to 1/2 chip, allowing a balance between noise robustness and accurate code phase alignment. The pseudorange accuracy is constrained by the discrete shifting of PRN replicas in Simulink, which only allows integer sample adjustments. A filter accumulates fractional shifts ($\frac{1}{4}$ per iteration) until a full sample shift is applied. However, the process stabilizes at 3/4 of the incoming sample variation, limiting accuracy to 18.32 m.

6. Results

6.1. Acquisition Performance

The acquisition stage successfully identified the incoming signal and provided an initial estimate

of the code phase delay, ensuring that the tracking loop started with an accurate initialization. To prevent ambiguities in delay estimation, the convolution process was extended over two PRN code sequences. This accounted for cases where the initial delay exceeded the PRN sequence length, a scenario particularly relevant in VULCAIN's mission profile. The acquisition process, lasting 1 ms, was sufficiently fast to ensure that range variations did not exceed the DLL pull-in range, preventing tracking divergence.

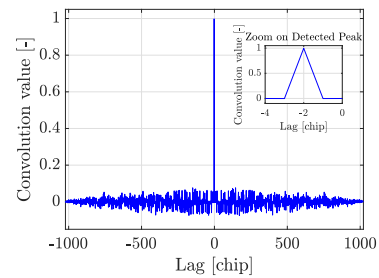


Figure 2: Convolution process result in the acquisition module

6.1.1 Code Tracking Loop Performance

The DLL demonstrated the ability to track the incoming code phase with an accuracy of 0.25 sample, consistent with the receiver's sampling constraints. However, discretization errors introduced a residual range uncertainty of approximately ± 36.64 m, as shown in Figure 3, doubling the expected error. When increasing the sampling frequency to 8.184 MHz, the uncertainty was reduced to ± 22.89 m, as presented in Figure 4, confirming the importance of a high sampling rate for improving pseudorange precision.

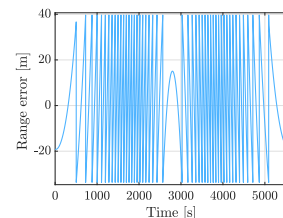


Figure 3: Code tracking error tracking error, $f_s = 4.092$ MHz

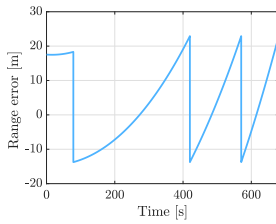


Figure 4: Code tracking error tracking error, $f_s = 8.184$ MHz (for a limited temporal window)

6.1.2 Carrier Tracking Performance

The carrier tracking loop, composed of independent PLL and FLL, was first model without the navigation bit transitions and the ranging code. For this reason, at this stage, the PLL discriminator was set as *atan2*. The carrier tracking model exhibited different performances depending on the sampling frequency. As shown in Figure 7, at 4.092 MHz, the PLL struggled due to integer ambiguity and phase jumps caused by Doppler variations, leading to errors accumulating over time. When increasing the sampling frequency to 40.92 MHz, as presented in Figure 8, tracking accuracy significantly improved, demonstrating that higher-resolution sampling is crucial for reliable carrier phase estimation. However, the frequency tracking loop effectively tracks the Doppler shift for both analyzed sampling frequencies, as observed in Figure 5 and Figure 6. For carrier tracking, each loop is assisted by a second-order filter. The filter bandwidth for frequency tracking is set lower than that of the phase filter, at 7.5 Hz, to reduce frequency tracking errors and limit long-term phase error accumulation. In contrast, the phase filter operates with a 14 Hz bandwidth to stabilize the phase loop, accepting higher estimation uncertainty as a trade-off. For both filters, the damping factor is set to 0.7071, a common choice in control systems to prevent undershooting and excessive oscillations.

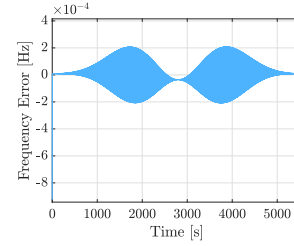


Figure 5: Frequency tracking error, $f_s = 4.092$ MHz

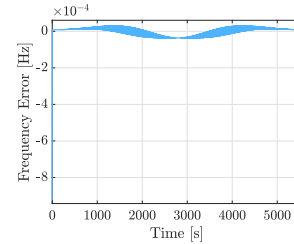


Figure 6: Frequency tracking error, $f_s = 4.092$ MHz

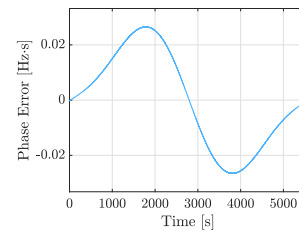


Figure 7: Phase tracking error, $f_s = 4.092$ MHz

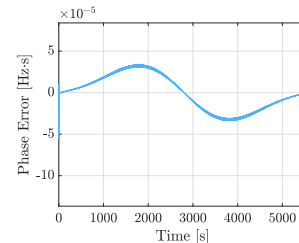


Figure 8: Phase tracking error, $f_s = 4.092$ MHz

6.1.3 Complete Tracking Loop Integration

The fully integrated code and carrier tracking loops were implemented with the *Costas* discriminator for the PLL to be insensitive to navigation bit transitions. It maintained consistent pseudorange estimates, demonstrating that the code loop remained unaffected by carrier tracking divergence, as expected from the selected normalized early-minus-late discriminator. However, carrier loop instabilities are observed in Figure 9 and Figure 10 due to the FLL discriminator's sensitivity to navigation bit transitions, which caused accumulating frequency es-

timation jumps.

Another critical aspect of the integrated tracking process was the interaction between code and carrier loops. Each time the DLL updated its estimate to track code phase variations, it briefly disturbed the carrier loop, introducing small tracking oscillations. In future implementations, these transient effects could be mitigated with advanced loop filters or hybrid tracking approaches.

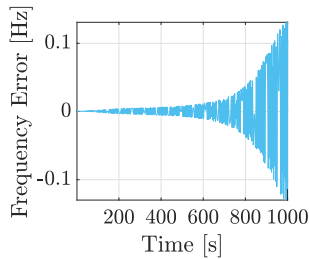


Figure 9: Frequency tracking error

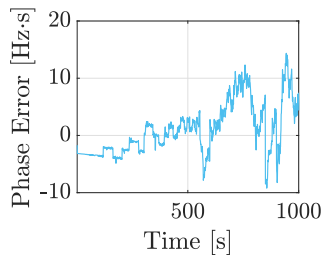


Figure 10: Phase tracking error

6.1.4 Navigation Message Recovery

Despite challenges in carrier tracking, the navigation message was successfully recovered as presented in Figure 11. To compensate for carrier tracking instabilities, an adaptive integration process was used, accumulating signal energy over 20 ms in both in-phase and quadrature components. This ensured correct bit sequence extraction, even in the presence of partial carrier misalignment.

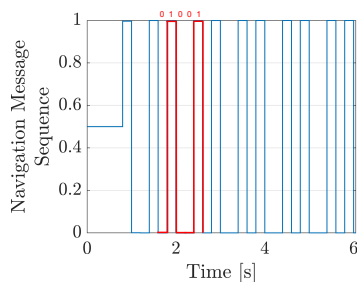


Figure 11: Recovered Navigation sequence

7. Conclusions

This thesis designed and evaluated a radio-frequency inter-satellite link for autonomous one-way ranging within the VULCAIN mission framework, analyzing key receiver parameters such as sampling frequency, discriminator selection, and filtering techniques. A comprehensive system model was successfully developed, adapting GNSS receiver architectures for formation flying and proving the feasibility of precise one-way ranging. However, carrier tracking loop divergence was identified as a critical limitation, requiring further refinement.

8. Bibliography

References

- [1] Kai Borre, Dennis M. Akos, Nicolaj Bertelsen, Peter Rinder, and Søren Holdt Jensen. *A Software-Defined GPS and Galileo Receiver: A Single-Frequency Approach*. Birkhäuser, Boston, MA, USA, 2007.
- [2] B. Hofmann-Wellenhof, H. Lichtenegger, and E. Wasle. *GNSS- Global Navigation Satellite Systems -GPS, GLONASS, Galileo, and more*. Aerospace Engineering. Springer, 2007.
- [3] Win Kay Khaing, Zaw Min Naing, Su Su Yi Mon, Aung Soe Khaing, Hla Myo Tun, and Sao Hone Pha. Implementation of code and carrier tracking loops for software gps receivers. *International Journal of Scientific & Technology Research*, 4(6):6–12, 2015.